# Charge Extraction From $TiO_2$ Nanotubes Sensitized With CdS Quantum Dots by SILAR Method

Cecilia I. Vázquez, Ana M. Baruzzi, and Rodrigo A. Iglesias

***Abstract*—Quantum dot (QD) solar cells based on different materials have received a noticeable interest during the past ten years; however, their efficiency and stability are still the main drawback of this technology, which leads to a lack of performance of these devices. There are several electron loss (and efficiency) processes involved after photon absorption, but perhaps the main issue is with the electron recombination after excitation of the surface. In this paper, we have studied the dependence of short-circuit photocurrent of $TiO_2$ nanotubes with varying amounts of CdS QDs deposited by the successive ionic layer adsorption and reaction method. We have found that there is an optimum coverage of CdS in order to achieve the maximum photocurrent value. This behavior is explained and characterized in terms of prevailing recombination processes at higher CdS coverage, where quantum confinement becomes less important. By using the charge extraction method, we could determine the time dependence of electrode charge and indicates that the back reaction of electrons with the redox electrolyte present in solution is of the first order in electron density and that it originates from the electrons present in the $TiO_2$ conduction band.**

***Index Terms*—Charge extraction, open circuit, solar cells, successive ionic layer adsorption and reaction (SILAR).**

## I. Introduction

NANOSTRUCTURED semiconductors have received great attention in the development of solar cells; particularly since the pioneering works of Grätzel on dye sensitized solar cells (DSSC), a huge number of research topics have been directed to the optimization of the different parts of DSSC. Recently, as an emergent alternative to this device, quantum dot sensitized solar cells (QDSC) have been realized. This case involves the optical sensitization of nanostructured $TiO_2$ with nanocrystals of CdS [1], [2], CdSe [3], [4], CdTe [5], PbS [6], among others, where the efficiency is supposed to be enhanced because of the strong quantum confinement and the chance of having multiple exciton generation on these sensitizers. Even so, the efficiency of QDSC is still far from the theoretical estimations and, moreover, below the maximum efficiency reached with DSSC [7].

It has been recognized that $TiO_2$ nanotubes improve the electron transport by vectorization of the electron diffusion but in detriment of a lower specific surface when compared with nanoparticles, reducing the sensitizer loading. On the other side, the CdS nanocrystals show a reasonably good energy coupling with $TiO_2$ and an enhancement of photocurrents with increased loading; however, a huge loading with quantum dots (QDs) implies clusterization and faster self-recombination. There are several methods to prepare QDs [8], [9]; however, SILAR is simple, less expensive, less time consuming, and prone to automatization [10]. Besides, the lack of organic ligands on its synthesis and direct QDs precipitation onto the substrate surface ensures an intimate contact between both surfaces, favoring electron injection [11].

One of the main issues leading to a reduced efficiency in QDSC is electron recombination with the electrolyte in contact with the nanostructured surface. Cameron and Peter [12] have proposed a method to study the kinetic of electron recombination with the electrolyte, i.e., at open circuit, which can give information related to the different recombination processes responsible of the decrease in efficiency at short circuit.

Considering the previous aspects, we evaluate kinetic information of the different recombination processes that can take place in surfaces composed of $TiO_2$ nanotubes covered with CdS nanoclusters. Specifically, we have varied the CdS coverage and size of nanotubes. We found that there is an optimum coverage because of loss of quantum confinement at high CdS loads. Kinetic data were analyzed in terms of varying CdS coverage and nanotube length for the same amount of sensitizer, and we found a single electron back reaction process arising from the conduction band of $TiO_2$ with the solution redox electrolyte. Particularly, this rate determining step has relaxation times on the order of $10^1$ s.

## II. Experimental Details

### A. Materials

Titanium foil was purchased from Sigma Aldrich. Ammonium fluoride ($NH_4F$), ethylene glycol (Dorwil), cadmium acetate 2-hydrate (Anedra), and sodium sulfide nonahydrate (Tetrahedron) were used as received to prepare the CdS|$TiO_{2\text{-NT}}$ sensitized surface. All solutions were prepared with ultrapure water (Mili Q-Mili RO system).

### B. Fabrication of $TiO_2$ Nanotube Surfaces

Self-organized $TiO_{2\text{-NT}}$s were fabricated by anodization of Ti foils in ethylene glycol (94.5 wt %) solution with additions of 0.3 wt % of $NH_4F$ and 4.0 wt % of deionized (DI) water.

Manuscript received April 4, 2016; revised August 3, 2016 and September 2, 2016; accepted September 15, 2016. Date of current version October 19, 2016. The work of C. I. Vázquez was supported by CONICET through a postdoctoral fellowship. This work was supported in part by the Secretaría de Ciencia y Técnica, Facultad de Ciencias Químicas, Universidad Nacional de Córdoba (SeCyT UNC); in part by Consejo Nacional de Investigaciones Científicas y Técnicas; and in part by Agencia Nacional de Promoción Científica y Tecnológica.

The authors are with the INFIQC CONICET, Departamento de Fisicoquímica, Facultad de Ciencias Químicas, Universidad Nacional de Córdoba, Córdoba 5016, Argentina, and also with Ciudad Universitaria, Córdoba 5000, Argentina (e-mail: cvazquez@fcq.unc.edu.ar; abaruzzi@fcq.unc.edu.ar; riglesias@fcq.unc.edu.ar).

This paper has supplementary downloadable material available at http://ieeexplore.ieee.org.

Color versions of one or more of the figures in this paper are available online at http://ieeexplore.ieee.org.

Digital Object Identifier 10.1109/JPHOTOV.2016.2611656

Prior to the anodization, Ti foils were ultrasonically cleaned successively in acetone, isopropanol, ethanol, and DI water to remove impurities. The foils were subsequently rinsed with DI water and then dried in an $N_2$ stream. To obtain $TiO_{2\text{-NT}}$, the degreased Ti foil ($1.0 \times 1.0 \times 0.05$ cm$^3$ in size) was immersed in the electrolyte. Anodization was carried out in a two electrode cell, with a platinum (Pt) foil cathode, at 40 V under controlled temperature (24°C) with constant magnetic stirring. After a certain amount of time for anodization (1, 2, 4, 6 or 10 h), the sample was removed from the electrode cell and washed in an ultrasonic bath for 30–60 s in DI water or for 5 min in ethanol to remove the surface debris. A subsequent annealing at 400 °C for 2 h with a temperature ramp rate of 5 °C$\cdot$ min$^{-1}$ in air was applied to achieve the crystallization of $TiO_{2\text{-NT}}$ before the CdS deposition.

### C. Modification of $TiO_2$ Surfaces With CdS

CdS QDs were deposited on the $TiO_{2\text{-NT}}$ by the successive ionic layer adsorption and reaction (SILAR) method. One SILAR cycle consists of the following four steps: $TiO_{2\text{-NT}}$ were sequentially dipped for:

1) 40 s in 0.005 M cadmium acetate ($Cd(Ac)_2$);
2) 1 min in DI water;
3) 40 s in 0.005 M sodium sulfide ($Na_2S$);
4) 1 min in DI water.

All solutions were under continuous agitation at room temperature. Such an immersion procedure was repeated for different number of cycles, producing yellow to orange samples.

### D. CdS Removal From the $TiO_2$ Surface

CdS QDs were removed from the $TiO_{2\text{-NT}}$ surface by immersion in 1 M $HNO_3$ solution with continuous agitation over 6 h in order to promote the dissolution reaction

$$3CdS_{(s)} + 8HNO_{3(aq)} \rightarrow 3Cd(NO_3)_{2(aq)} + 2NO_{(g)} + 3S_{(s)} + 4H_2O_{(l)}.$$

Under these conditions, the cleaned $TiO_{2\text{-NT}}$ electrode is stable [13]. After that, the electrode surface was rinsed and dipped for 5 min in DI water and dried with $N_2$ stream. A subsequent annealing at 400 °C for 2 h with a temperature ramp rate of 5 °C$\cdot$min$^{-1}$ in air was applied to eliminate the remaining $S_{(s)}$ from the electrode surface. This way, the $TiO_{2\text{-NT}}$ electrodes can be used repeatedly.

### E. Measurements

The electrochemical and photoelectrochemical experiments were carried out in a conventional spectrophotometric cuvette, especially adapted to hold a three electrode cell configuration, using a platinum wire as counter electrode and a $Ag|\,AgS_{(s)}|\,Na_2S_{(aq,1M)}$ as reference electrode. All potentials are relative to the open-circuit potential (OCP) under darkness. Photoelectrochemical measurements were conducted using an Autolab PGSTAT101 potentiostat/galvanostat. Photoanodes were illuminated with a collimated, via an optical fiber, UV-filtered light source (Kratos LH-150/l 150 W Xe) with a circular spot of 0.20 cm$^2$. Photocurrent action spectra were measured using a bandpass filter covering 380–560 nm. All photoelectrochemical measurements were done at room temperature in a freshly prepared 1 M $Na_2S$ solution.

Charge extraction method, developed by Duffy *et al.* [14] and explained in more detail in Section III-C, was used under the following experimental conditions: Initially, the cell was at OCP under darkness during 50 s; after that, it was suddenly illuminated during 50 s, and then, the light was interrupted. After certain period of time at OCP (from 2 to 150 s), the cell was short-circuited at a potential 30–50 mV more positive than the initial OCP under darkness ($\Delta E_{\text{ext}}$) and the current measured during 0.2 s obtaining an *i–t* profile. The chronoamperometric curve was integrated and the extracted charge was obtained. After the measure was repeated for different intervals of time, a dark current profile was performed by waiting 100 s in darkness at OCP and short-circuiting the cell at the same $\Delta E_{\text{ext}}$ used before; this extracted charge was subtracted from all previous points to take account of the capacitance and parasitic currents of the electrochemical interface.

The topology of the electrode surface was characterized using a field-emission scanning electron microscope (SEM) operating at 8 kV (Sigma-Zeiss, LAMARX Laboratories, Córdoba, Argentina). Energy-dispersive X-ray spectrometers (AZTec-Oxford) fitted to the electron microscope were used for elemental analysis.

## III. Results and Discussion

### A. Sample Characterization

$TiO_{2\text{-NT}}$ electrodes were prepared by Ti foil anodization at 40 V and 24 °C during different anodization times. Detailed analysis of cross-sectional and face-on SEM micrographs revealed that the only geometric parameter that changes significantly from sample to sample is the tube length (see supporting information). Wall thickness ($(25 \pm 8)$ nm), tube diameter $\left((8 \pm 3) \times 10^1\ \text{nm}\right)$, and tube packing are relatively constant across all samples. In consequence, surface area depends almost exclusively on the nanotube length.

### B. Effect of CdS Coverage on the Photoelectrochemical Response of $CdS|TiO_{2\text{-NT}}$

The current–potential (*I–V*) curves characteristics of $CdS|TiO_{2\text{-NT}}$ electrodes prepared with different number of SILAR cycles are presented in Fig. 1(a). All experiments were performed in with the same $TiO_{2\text{-NT}}$ surface after removing CdS using the cleaning methodology described in Section II-D. The electrochemical measurements were carried out in 1 M $Na_2S$, i.e., an efficient hole scavenger, because of the stability of the electrodes in this electrolyte [15]. The informed potential was corrected according to each electrode OCP under darkness.

From 2 to 25 SILAR cycles, the $I_{\text{sc}}$ (short-circuit current), $V_{\text{oc}}$ (photopotential), and fill factor (FF) increase progressively because of the higher amount of sensitizer deposited over the $TiO_{2\text{-NT}}$ surface, resulting in a better photon harvesting, charge separation, and electron accumulation [16]; however, 10

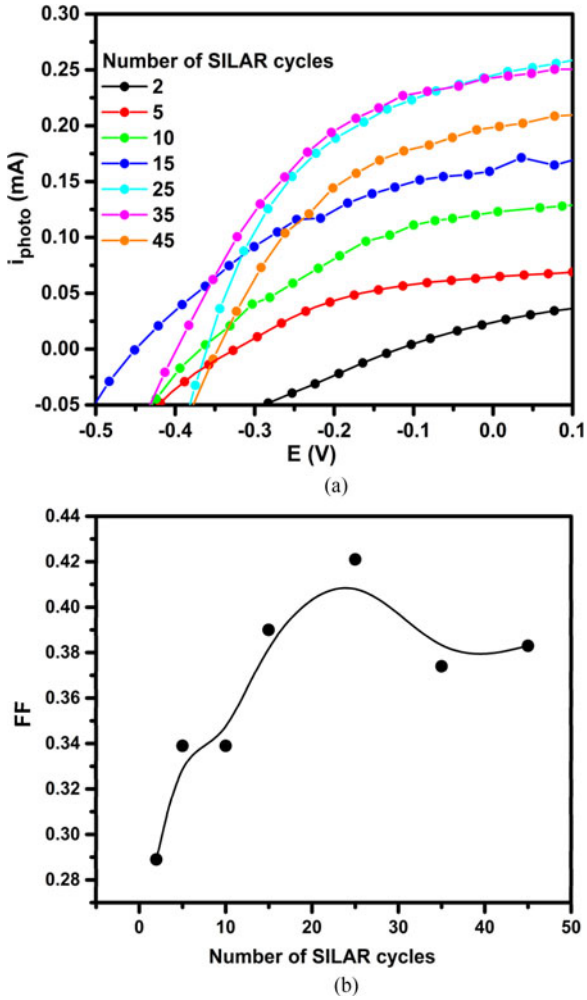


Fig. 1. (a) *I–V* profiles of CdS|$TiO_{2\text{-NT}}$ electrodes containing different amounts of CdS. (b) FF dependence on number of SILAR cycles. $TiO_{2\text{-NT}}$ length: (3.5 $\pm$ 0.2) $\mu$m. Solid lines are B-Spline fittings of the experimental data.

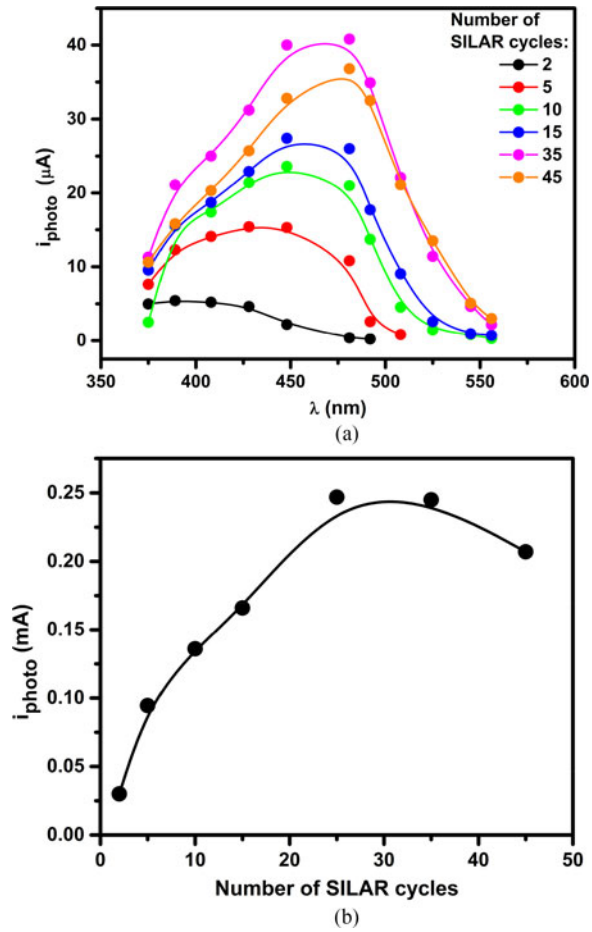


Fig. 2. (a) Photocurrent action spectra of CdS|$TiO_{2\text{-NT}}$ electrodes containing different amounts of CdS. (b) Dependence of $i_{\text{photo}}$ on the SILAR cycles of CdS deposition under white light illumination. $TiO_{2\text{-NT}}$ length: (3.5 $\pm$ 0.2) $\mu$m. Solid lines are B-Spline fittings of the experimental data.

additional SILAR cycles to the electrode (35 cycles in total) produce a slight decrease of the $I_{\text{sc}}$ and FF [see Fig. 1(b)] values, indicating that there is an optimal number of SILAR cycles (i.e., surface coverage) to attain a maximum photovoltaic conversion efficiency.

The ability of the deposited CdS as a sensitizer was evaluated by measuring the photocurrent action spectra of $TiO_{2\text{-NT}}$ electrodes containing different amounts of CdS [see Fig. 2(a)]. In addition, Fig. 2(b) shows the photocurrent evolution with the number of SILAR cycles with white light illumination. As the number of SILAR cycles (from 2 to 35 cycles) increases, so does the amount of adsorbed CdS|$TiO_{2\text{-NT}}$ enhancing the initial current as expected. At the same time, the maximum current is shifted to higher wavelengths (from 390 to 480 nm) due to quantum confinement, indicating that a greater amount of CdS also leads to an increase of the number and average particle size of the CdS clusters [17]. However, with a further increase in the load of CdS, ranging from 35 to 45 SILAR cycles, the maximum photocurrent starts to decrease with an almost negligible shift toward higher wavelengths. This indicates that the effect of quantization is lost and the subsequent addition of CdS enhances the back recombination of electrons, favoring this way undesirable side paths, such as recombination of excitons in the CdS, reaction of electrons with the oxidized species in the sulfide solution, or fall in trap states present in the forbidden gap of the semiconductor. As consequence, there is a maximum photocurrent value indicating that an optimal number of SILAR cycles can be achieved. In this experimental arrangement, the maximum conversion efficiency is attained at about 30 SILAR cycles, and it is worth remarking that this value also matches the maximum FF in Fig. 1(b).

To ensure that the amount of CdS in the $TiO_2$ surface increases continuously with the number of SILAR cycles, the composition of CdS|$TiO_{2\text{-NT}}$ was further investigated by the energy-dispersive X-ray spectroscopy (EDS) analysis (see Fig. 3). It is clear from Fig. 3 that the amount of CdS increases, even for high CdS coverage (i.e., 40 SILAR cycles), where the photocurrent decreases. Although the Cd:S atomic ratio cannot be directly obtained from the intensity of the EDS spectra shown in Fig. 3 [18], it can be noticed that the Cd:S ratio remains constant when the coverage increases.

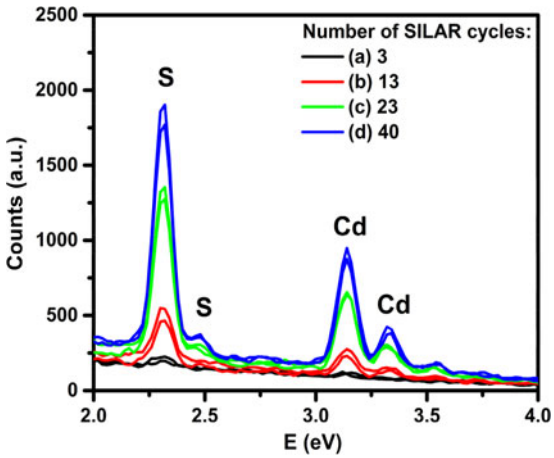


Fig. 3. EDS spectra of CdS|$TiO_{2\text{-NT}}$ electrodes containing different amounts of CdS. The spectra were taken with the detector on top of the sample surface. Number of SILAR cycles: (a) 3, (b) 13, (c) 23, and (d) 40. Two spectra with the same color are shown, which in turn correspond to different locations on the surface of the same CdS|$TiO_{2\text{-NT}}$ surface. $TiO_{2\text{-NT}}$ synthesis conditions: 40 V, 24 °C, and 8 h.

In order to have a qualitative view of the CdS distribution along the nanotubes, Fig. 4 shows EDS color maps taken with the detector pointing to the side of nanotube walls.

Fig. 4(a) shows a $TiO_{2\text{-NT}}$ surface modified with three SILAR cycles. The amount of CdS deposited is so small that the equipment can hardly distinguish it from the $TiO_2$ surface. When adding ten more SILAR cycles [see Fig. 4(b)], there is a slight increase of pink pixel density (Cd atoms) in the $TiO_{2\text{-NT}}$ region when compared with the bare Ti surface (light blue). When the number of SILAR cycles is increased to 23 [see Fig. 4(c)], the upper half of the $TiO_{2\text{-NT}}$s is clearly covered up and with further increase of the deposited CdS amount up to 40 SILAR cycles, homogeneous distribution of Cd and S atoms throughout the length of $TiO_{2\text{-NT}}$ is observed.

This implies that the $TiO_{2\text{-NT}}$ filling is not homogeneous with the number of SILAR cycles, i.e., the deposit initially begins in the nanotube entrance, and as long as the amount of CdS is increased, it also covers the bottom of the NT. Therefore, depending on the nanotube length, there will be different QD sizes at different heights. In other words, if the $TiO_{2\text{-NT}}$ are too short, all the deposited CdS clusters will have approximately the same size along the NT surface, but if they are longer, as in Fig. 4, the deposition is promoted at the top of the nanotubes and increasing the SILAR cycles number the deposition occurs also at the NT bottom concomitant with the growing at the entrance of the nanotubes resulting in a sort of "progressive" cluster size distribution. These results can also be noted in Fig. 2: When a little amount is deposited (for example, two SILAR cycles), the photocurrent generation varies between 370 and 450 nm approximately with a maximum at 400 nm; however, with large CdS quantities, such as 35 SILAR cycles, the photocurrent is practically generated in the whole spectrum range (between 370 and 560 nm), and the photocurrent maximum is wide, which is a clear indication of the large distribution of cluster sizes. As much as the CdS coverage increases the location of the photocurrent maximum and onset shift toward higher wavelengths [see Fig. 2(a)], it indicates the quantum confinement disappearance given by an increase of the cluster size. These results are promising to a given extent because using a certain number of SILAR cycles (in this case 30, where both the photocurrent and its generation wavenumber range are maxima), these photoelectrodes are capable of convert photons of a large wavelength range in the visible region, increasing the "usable" portion of the solar spectra, resulting in a sort of "rainbow" solar cell, like it was proposed by Kamat *et al.* [19]. However, the number of SILAR cycles has to be optimized; a large CdS deposit leads to a bulk behavior with the consequent photocurrent efficiency decay, which is a situation clearly noted when more than 45 SILAR cycles are performed [see Fig. 2(b)].

### C. Charge Extraction Method of CdS|$TiO_{2\text{-NT}}$ Electrodes

In order to study the electron back reaction process with the electrolyte in CdS|$TiO_{2\text{-NT}}$ surfaces, the charge extraction technique developed by Duffy *et al.* was used [14]. When the solar cell is illuminated under open-circuit conditions, and then the potential is left to decay in the darkness, the excited electrons can follow several paths (see Fig. 5), namely

1) exciton recombination ($k_r$);
2) injection of $e^-_{\text{CdS}}$ into the $TiO_2$ conduction band ($k_0$);
3) back reaction of $TiO_2$ with the electrolyte ($k_1$);
4) back reaction of $e^-_{\text{CdS}}$ with the electrolyte ($k_2$).

Several variables could influence the different $k_n$ values, such as incident light intensity, electron diffusion, and the presence of trap states in the $TiO_{2\text{-NT}}$ and CdS QDs [12], [20], the quality of the electric contact between them, the potential barrier between the semiconductors and the redox species adsorbed on its surface, as well as temperature, concentration, diffusion, and convection of the electrolyte [21], among others. In this analysis, all the measurements were performed with the same experimental setup, changing only the CdS amount or $TiO_{2\text{-NT}}$ length; nevertheless, all the reported kinetic results should be consider "apparent" or "effective" and the time constant values as global data influenced mainly by the CdS coverage and the $TiO_{2\text{-NT}}$ length.

In the charge extraction method, the surface is initially illuminated at an open-circuit until the stationary condition of the photopotential, this is when the rates for photogeneration and back reaction of photoelectrons become equal. Then, the light is interrupted, and the potential (and charge accumulated in the electrodes) is allowed to decay for certain time after which the cell is short-circuited and the remaining accumulated charge flows through the external circuit, as shown in the inset of Fig. 6(a). Under short-circuit conditions, the collection efficiency for electrons approaches to unity, therefore the back reaction is negligible mainly due to the different timescale for each process [12], [22]. The remaining charge accumulated in the conduction band of the semiconductor can be integrated from current-time profiles. Performing the charge extraction method at different intervals of time in darkness, the electron concentration decay over time can be determined, as shown in Fig. 6(a) and (b).

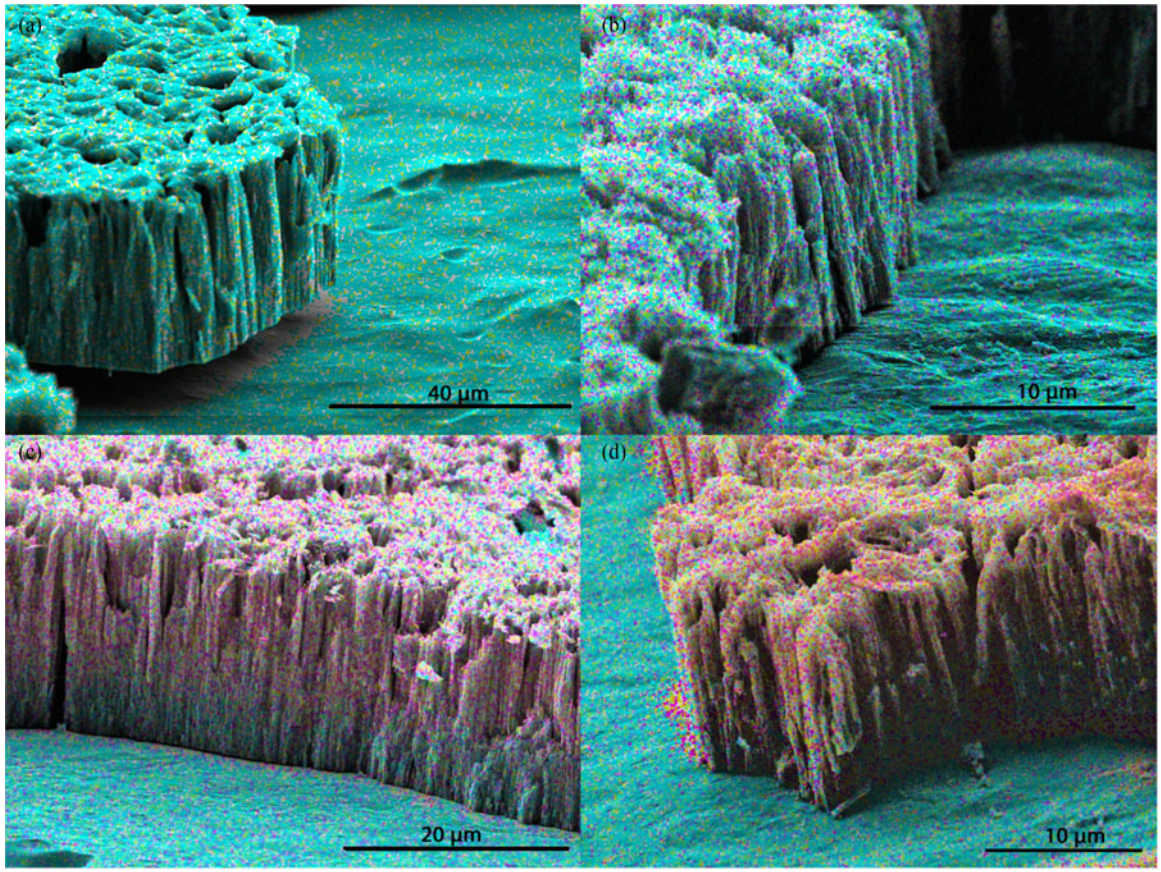


Fig. 4. SEM-EDS elemental mapping of CdS|$TiO_{2\text{-NT}}$ electrodes containing different amounts of CdS. Number of SILAR cycles: (a) 3, (b) 13, (c) 23, and (d) 40. $TiO_{2\text{-NT}}$ synthesis conditions: 40 V, 24 °C, and 8 h. Reference: Blue stands for Ti, yellow for S, and pink for Cd. O is not displayed for figure clarity.

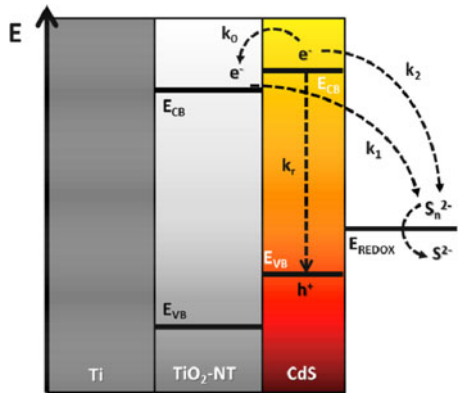


Fig. 5. Energy band diagram of CdS|$TiO_{2\text{-NT}}$ showing the main recombination paths of excited electrons.

In that direction, we performed two series of experiments: 1) using the same $TiO_{2\text{-NT}}$ surface with different amounts of CdS [such as in Section III-B, Fig. 6(a)] and 2) using nanotubes of different length and the same amount of CdS, i.e., five SILAR cycles [see Fig. 6(b)].

As can be noted in Fig. 6(a), the different experiments for the same surface are quite reproducible, because all *E–t* profiles can be perfectly superimposed. All the experiments [see Fig. 6(a) and (b)] show a first-order decay reaction kinetics, and the $Q$ versus $t$ data can be fitted with a simple exponential function, as in

$$Q(t) = A_0 + A_n e^{-t/\tau_n} \tag{1}$$

where $\tau_n$, which is the apparent lifetime of electrons present in the conduction band, can in turn be related to the kinetic constants shown in Fig. 5 as

$$\tau_n = \frac{1}{k_n}. \tag{2}$$

The results obtained from both kinds of experiments, i.e., variation of CdS coverage and modification of NT length, are shown in Fig. 7, with orders of magnitude similar to previous reports [20].

In the *I–V* curves and photocurrent action spectra shown above, we have found a direct relation between the number of SILAR cycles and photoelectrochemical response for the same $TiO_{2\text{-NT}}$ surface. However, in Fig. 7(a), there is not a noticeable dependence of $\tau_n$ on the CdS deposited amount on the same electrode; therefore, it seems that the back reaction kinetics of electron recombination does not depend on sensitizer size or surface concentration. On the other hand, when the size and concentration of the CdS QDs is kept approximately constant [five SILAR cycles, Fig. 7(b)], and the $TiO_2$ nanotube length

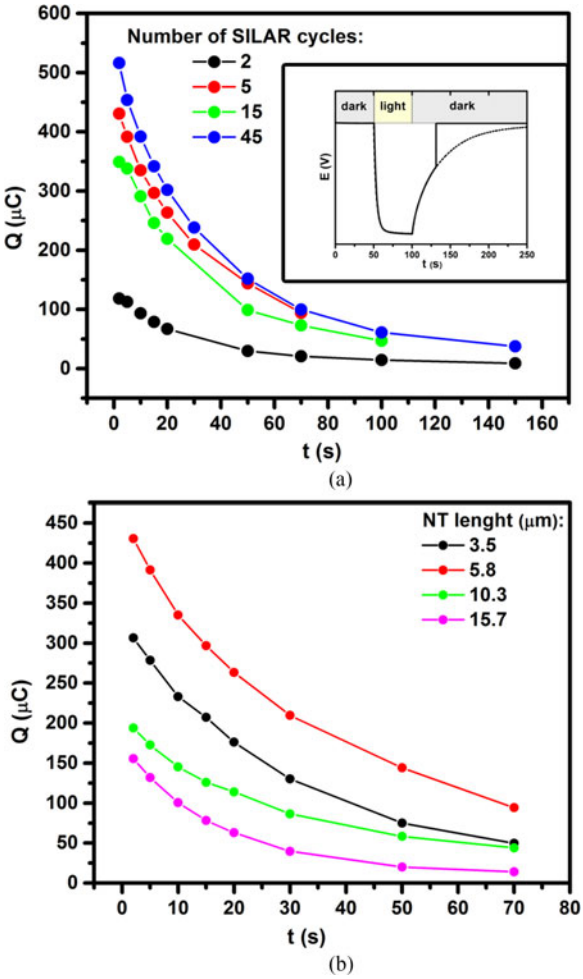


Fig. 6. (a) Extracted charge from CdS|$TiO_{2\text{-NT}}$ electrodes with different number of SILAR cycles. $TiO_{2\text{-NT}}$ length: $(3.5 \pm 0.2)$ $\mu$m. (Inset) Photopotential–time curves interrupted at two different decay times by shortcircuiting the cell for CdS|$TiO_{2\text{-NT}}$ electrodes with 45 SILAR cycles. (b) Extracted charge from CdS|$TiO_{2\text{-NT}}$ electrodes with five SILAR cycles and different $TiO_{2\text{-NT}}$ length.

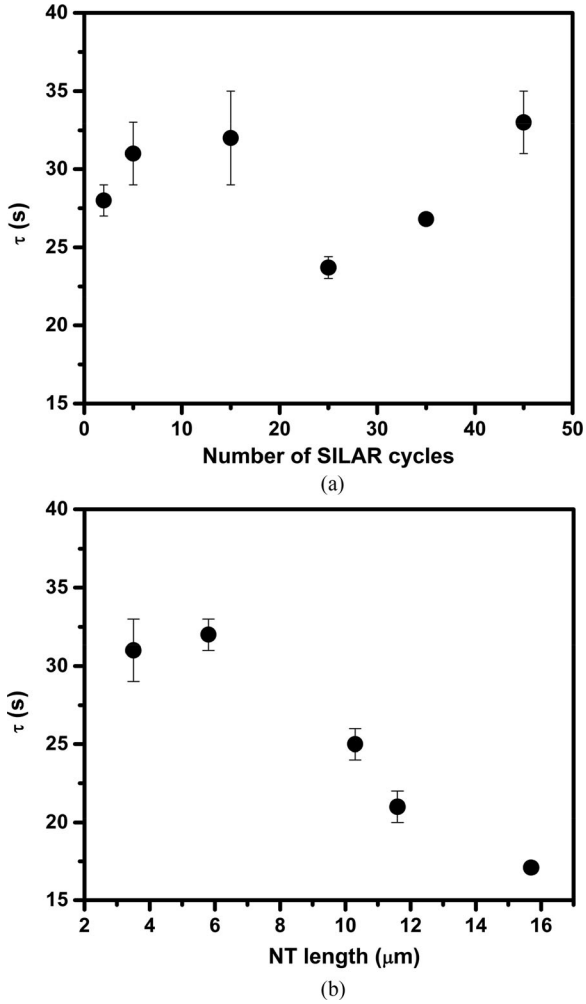


Fig. 7. Apparent electron lifetime as a function of (a) number of SILAR cycles for deposition of CdS at a $TiO_{2\text{-NT}}$ with an average length of $(3.5 \pm 0.2)$ $\mu$m and (b) $TiO_{2\text{-NT}}$ length with a CdS coverage given by five SILAR cycles.

is changed, there is a sustained decrease of $\tau_n$. These results indicate that the back reaction from the $TiO_2$ conduction band ($k_1$) is the rate determining step instead of the back reaction from sensitizer's conduction band ($k_2$). Therefore, $k_0 \gg k_2$ as it has been recently reported in bibliography by Nakamura *et al.*, who found that the electron injection from the optical sensitizer into $TiO_2$ conduction band is on the order 1–9 ps [23].

From a photon conversion efficiency point of view, it is desirable that the back reaction process would be as slow as possible in order to increase the number of captured electrons by the Ti electric contact. As it was shown, the back reaction process occurs from the $TiO_2$ conduction band and not from the CdS QDs, and therefore, the presence of a thin blocking layer in the CdS|$TiO_{2\text{-NT}}$ surface will not affect the CdS–$TiO_2$ contact and could avoid electron recombination paths with the electrolyte solution. One possibility is posttreatment with $TiCl_4$, as it was performed by Kim *et al.* [24], to passivate defects on the $TiO_2$ electrode surface with a new $TiO_2$ coating layer that could also avoid CdS photodegradation.

## IV. Conclusion

In this paper, we found that photocurrents attained from CdS sensitized $TiO_2$ nanotubes reach a maximum for a given CdS coverage. This coverage can be tuned by using SILAR synthesis, this way keeping control over the number of cycles performed, hence the coverage. The optimal CdS amount should be deposited to avoid quantum confinement loss and the consequent decay of the cell efficiency. Besides, a large particle size distribution along the nanotube is important to obtain photoelectrodes that are able to convert photons of a large wavelength range in the visible region, increasing the available portion of the solar spectra.

By using the charge extraction method, we were able to determine that the bottleneck step in the back reaction between the excited electrons and the redox electrolyte is the recombination of electrons from the $TiO_2$ conduction band.

## Acknowledgment

The authors would like to thank the LAMARX Laboratory for the scanning electron microscopy and fruitful discussions.

## REFERENCES


[1] Y. Medina-Gonzalez, W. Z. Xu, B. Chen, N. Farhanghi, and P. A. Charpentier, "CdS and CdTeS quantum dot decorated $TiO_2$ nanowires. Synthesis and photoefficiency," *Nanotechnol.*, vol. 22, 2011, Art. no. 065603. doi:10.1088/0957-4484/22/6/065603.

[2] W.-T. Sun *et al.*, "CdS quantum dots sensitized $TiO_2$ nanotube-array photoelectrodes," *J. Amer. Chem. Soc.*, vol. 130, pp. 1124–1125, 2008. doi:10.1021/ja0777741.

[3] A. Kongkanand, K. Tvrdy, K. Takechi, M. Kuno, and P. V Kamat, "Quantum dot solar cells. Tuning photoresponse through size and shape control of CdSe-$TiO_2$ architecture," *J. Amer. Chem. Soc.*, vol. 130, pp. 4007–4015, 2008. doi:10.1021/ja0782706.

[4] I. Robel, M. Kuno, and P. V Kamat, "Size-dependent electron injection from excited CdSe quantum dots into $TiO_2$ nanoparticles," *J. Amer. Chem. Soc.*, vol. 129, pp. 4136–4137, 2007. doi:10.1021/ja070099a.

[5] L. Jin, L. Shang, J. Zhai, J. Li, and S. Dong, "Fluorescence spectroelectrochemistry of multilayer film assembled CdTe quantum dots controlled by applied potential in aqueous solution," *J. Phys. Chem. C.*, vol. 114, pp. 803–807, 2010.

[6] J. Jean *et al.*, "ZnO Nanowire Arrays for Enhanced Photocurrent in PbS quantum dot solar cells," *Adv. Mater.*, vol. 25, pp. 2790–2796, 2013. doi:10.1002/adma.201204192.

[7] S. Rühle, M. Shalom, and A. Zaban, "Quantum-dot-sensitized solar cells," *ChemPhysChem*, vol. 11, pp. 2290–2304, 2010. doi:10.1002/cphc.201000069.

[8] G. H. Carey *et al.*, "Colloidal quantum dot solar cells," *Chem. Rev.*, vol. 115, pp. 12732–12763, 2015. doi:10.1021/acs.chemrev.5b00063.

[9] P. Sudhagar, E. J. Juárez-Pérez, Y. S. Kang, and I. Mora-Seró, *Low-Cost Nanomaterials: Quantum Dot-Sensitized Solar Cells*. London, U.K.: Springer-Verlag, 2014. doi:10.1007/978-1-4471-6473-9.

[10] D. S. Dhawale, D. P. Dubal, M. R. Phadatare, J. S. Patil, and C. D. Lokhande, "Synthesis and characterizations of CdS nanorods by SILAR method: Effect of film thickness," *J. Mater. Sci.*, vol. 46, pp. 5009–5015, 2011. doi:10.1007/s10853-011-5421-z.

[11] S. Giménez *et al.*, "Improving the performance of colloidal quantum-dot-sensitized solar cells," *Nanotechnol.*, vol. 20, pp. 295204–295210, 2009. doi:10.1088/0957-4484/20/29/295204.

[12] P. J. Cameron and L. M. Peter, "How does back-reaction at the conducting glass substrate influence the dynamic photovoltage response of nanocrystalline dye-sensitized solar cells?" *J. Phys. Chem. B.*, vol. 109, pp. 7392–7398, 2005. doi:10.1021/jp0407270.

[13] D. V Bavykin, A. A. Lapkin, J. M. Friedrich, and F. C. Walsh, "Acid transformation of $TiO_2$ nanotubes to nanoparticles," in *Proc. NSTI Nanotechnol. Conf.*, 2005, vol. 2, pp. 655–658.

[14] N. W. Duffy, L. M. Peter, R. M. G. Rajapakse, and K. G. U. Wijayantha, "A novel charge extraction method for the study of electron transport and interfacial transfer in dye sensitised nanocrystalline solar cells," *Electrochem. Commun.*, vol. 2, pp. 658–662, 2000. doi: 10.1016/S1388-2481(00)00097-7.

[15] L. Gerbino, C. I. Vázquez, A. M. Baruzzi, and R. A. Iglesias, "Effect of the electrolyte composition on the response of a $TiO_2$ | CdS-Based Photoanode," *Electrochim. Acta*, vol. 138, pp. 464–467, 2014.

[16] Y. Xie, G. Ali, S. H. Yoo, and S. O. Cho, "Sonication-assisted synthesis of CdS quantum-dot-sensitized $TiO_2$ nanotube arrays with enhanced photoelectrochemical and photocatalytic activity," *ACS Appl. Mater. Interfaces,* vol. 2, pp. 2910–2914, 2010. doi:10.1021/am100605a.

[17] N. Guijarro, T. Lana-Villarreal, Q. Shen, T. Toyoda, and R. Gómez, "Sensitization of titanium dioxide photoanodes with cadmium selenide quantum dots prepared by SILAR: Photoelectrochemical and carrier dynamics studies," *J. Phys. Chem. C.*, vol. 114, pp. 21928–21937, 2010.

[18] S. P. Limandri, M. A. Z. Vasconcellos, R. Hinrichs, and J. C. Trincavelli, "Experimental determination of cross sections for K-shell ionization by electron impact for C, O, Al, Si, and Ti," *Phys. Rev. A, Atomic, Mol. Opt. Phys.*, vol. 86, pp. 1–10, 2012. doi:10.1103/PhysRevA.86.042701.

[19] P. V. Kamat, "Quantum dot solar cells. Semiconductor nanocrystals as light harvesters," *J. Phys. Chem. C.*, vol. 112, pp. 18737–18753, 2008.

[20] J. R. Jennings, A. Ghicov, L. M. Peter, P. Schmuki, and A. B. Walker, "Dye-sensitized solar cells based on oriented $TiO_2$ nanotube arrays: Transport, trapping, and transfer of electrons," *J. Amer. Chem. Soc.*, vol. 130, pp. 13364–13372, 2008. doi:10.1021/ja804852z.

[21] V. Chakrapani, D. Baker, and P. V. Kamat, "Understanding the role of the sulfide redox couple (S2-/S(n)2-) in quantum dot-sensitized solar cells," *J. Amer. Chem. Soc.*, vol. 133, pp. 9607–9615, 2011. doi:10.1021/ja203131b.

[22] M. Bailes, P. J. Cameron, K. Lobato, and L. M. Peter, "Determination of the density and energetic distribution of electron traps in dye-sensitized nanocrystalline solar cells," *J. Phys. Chem. B.*, vol. 109, pp. 15429–15435, 2005. doi:10.1021/jp050822o.

[23] R. Nakamura, S. Makuta, and Y. Tachibana, "Electron injection dynamics at the SILAR deposited CdS quantum dot/$TiO_2$ interface," *J. Phys. Chem. C.*, vol. 119, pp. 20357–20362, 2015. doi:10.1021/acs.jpcc.5b06900.

[24] J. Kim *et al.*, "The role of a TiCl4 treatment on the performance of CdS quantum-dot-sensitized solar cells," *J. Power Sources,* vol. 220, pp. 108–113, 2012. doi:10.1016/j.jpowsour.2012.07.133.


Authors' photographs and biographies not available at the time of publication.